

 Open access • Journal Article • DOI:10.1103/PHYSREVD.14.1920

## Pseudoscalar mixing effects on hadronic and photonic decays of the new mesons

— [Source link](#) 

J. F. Bolzan, William F. Palmer, Stephen S. Pinsky

**Institutions:** Ohio State University

**Published on:** 01 Oct 1976 - Physical Review D (Ohio State Univ., Columbus (USA). Dept. of Physics)

**Topics:** Eta meson, Vector meson dominance, Meson and Pseudoscalar

Related papers:

- [Pseudoscalar glueball, the axial-vector anomaly, and the mixing problem for pseudoscalar mesons](#)
- [The low lying axial-vector mesons as dynamically generated resonances](#)
- [Charmonium: The model](#)
- [Mass spectrum of spin-zero mesons](#)
- [Pseudoscalar decay constants and eta. -->. 3. pi. in chiral and 1/N perturbation theory](#)

Share this paper:    

View more about this paper here: <https://typeset.io/papers/pseudoscalar-mixing-effects-on-hadronic-and-photonic-decays-3v13ke4scp>

Pseudoscalar Mixing Effects on Hadronic and  
Photonic Decays of the New Mesons\*

John F. Bolzan, William F. Palmer, and Stephen S. Pinsky

Department of Physics  
The Ohio State University  
Columbus, Ohio 43210

**MASTER**

Abstract

We calculate the mixing of  $\eta$ ,  $\eta'$ , and  $\eta_c$  in a cylinder dominated model and apply our results to the hadronic decay  $\psi' \rightarrow \psi\eta$  and a number of photonic decays, using vector meson dominance. The results are in excellent agreement with all experimental data.

NOTICE

This report was prepared as an account of work sponsored by the United States Government. Neither the United States nor the United States Energy Research and Development Administration, nor any of their employees, nor any of their contractors, subcontractors, or their employees, makes any warranty, express or implied, or assumes any legal liability or responsibility for the accuracy, completeness or usefulness of any information, apparatus, product or process disclosed, or represents that its use would not infringe privately owned rights.

\*Research supported in part by the U.S. Energy Research and Development Administration under contract AT(11-1)-1545.

## **DISCLAIMER**

**This report was prepared as an account of work sponsored by an agency of the United States Government. Neither the United States Government nor any agency Thereof, nor any of their employees, makes any warranty, express or implied, or assumes any legal liability or responsibility for the accuracy, completeness, or usefulness of any information, apparatus, product, or process disclosed, or represents that its use would not infringe privately owned rights. Reference herein to any specific commercial product, process, or service by trade name, trademark, manufacturer, or otherwise does not necessarily constitute or imply its endorsement, recommendation, or favoring by the United States Government or any agency thereof. The views and opinions of authors expressed herein do not necessarily state or reflect those of the United States Government or any agency thereof.**

## **DISCLAIMER**

**Portions of this document may be illegible in electronic image products. Images are produced from the best available original document.**

## 1. Introduction

In Refs.1, we have discussed Okubo-Zweig-Iizuka (OZI) Rule violation in the context of a model in which an intermediate state mediates the forbidden transitions. Unitarity requires this intermediate state; whether it is a cut (e.g.,  $\psi \rightarrow DD^* \rightarrow \rho\pi$  in  $\psi$  decay) or a real particle (a glue ball, an empty bag, an "O-meson," a closed string), it seems to be rather well parametrized by a pole in the  $J^P = 1^-$  and  $0^+$  channels we addressed in Refs.1, which included some of the more interesting decays of  $\psi$  and  $\psi'$  as well as the classical  $\phi \rightarrow \rho\pi$  rate.

This model will be extended here to OZI violating transitions in the  $0^-$  channel, which has been treated by several other authors.<sup>2-6</sup> The strikingly large  $\psi' \rightarrow \psi\eta$  rate, considering the small phase space, proves an interesting challenge for the model; furthermore, the model provides an interesting alternative to the treatment of Harari,<sup>2</sup> who finds a huge admixture of charm in  $\eta$  and  $\eta'$ , and encounters some problems with photonic decays. (Our results are summarized in Table II.)

Rooted in dual models and dual diagrams, the model<sup>7</sup> correlates deviations from the ideal mixing mass formula with deviation from ideal mixing in the states via an s-dependent interaction in the forbidden transition elements. In terms of dual diagrams the OZI forbidden process is one in which there is a U-turn, Fig.1a. If one views the quarks as being at the ends of a string, then this can be pictured as a closing of the string into a circle, which then re-opens, with equal probability, into any quark-antiquark state, according to SU(4) symmetry of the basic interaction. The closed string, or flux ring, sweeps out a cylinder, whose moving flux line boundaries, when cut, form tears in the cylinder bounded by quark lines which propagate in time the now open

flux lines, Fig.1b.

Within the framework of the topological expansion,<sup>8</sup> the cylinder diagrams are second order in a perturbation in higher and higher orders of the topology; the lowest order diagrams are the conventional planar graphs.

In this framework one associates the cylinder with the Pomeron singularity. Freund and Nambu,<sup>7</sup> in the context of a string picture, point out that both senses of flux circulation allow for both charge conjugations, and associate the  $2^{++}$ ,  $1^{--}$ ,  $0^{++}$  closed strings with the Pomeron trajectory or its daughters. We have used these objects in Refs.1 to study a number of OZI rule suppressions.

In all our previous work we have been careful not to restrict ourselves to a particular dynamical structure for the Pomeron and its associated singularities. It is our feeling that these objects are not simple poles even when we often treated them as such as a convenient approximation. In particular, the cylinder corrections may be Pomeron-Reggeon cuts, suggesting cylinders in all quantum number states which have Reggeons.

Moreover, if cylinders are established in the  $0^+$  and  $1^-$  channels, one can use a topological duality to infer the existence of a cylinder in the  $0^-$  channel. By topological duality we mean that topologically equivalent diagrams are dual in the usual sense. Consider for example the  $\psi - \phi\eta$  diagram. This is doubly suppressed and requires two cylinders, Fig.1c, which has the topology of a sphere with three holes with a particle attached at each hole. It is topologically equivalent to Fig.1d, which has an  $0^-$  cylinder. The line of argument is analogous to pinching an ordinary planar graph in different ways to infer existence of quark model states in s and t channels.

## 2. Mass-Degenerate Matrix

As a result of the cylinder correction in the  $0^-$  channel, the ideally mixed "planar" states will be mixed and the masses shifted.

We take the cylinder interaction to be

$$Q = \begin{bmatrix} 0 & 0 & 0 & \sqrt{2} f \\ 0 & 0 & 0 & f \\ 0 & 0 & 0 & f \\ \sqrt{2} f & f & f & 0 \end{bmatrix}$$

where the channels are  $\eta$ ,  $\eta'$ ,  $\eta_c$ , and  $0$ -meson, respectively. In second order this generates the interaction

$$0 = QPQ = \begin{bmatrix} \frac{2f^2}{s-m_0^2} & \frac{\sqrt{2}f^2}{s-m_0^2} & \frac{f^2}{s-m_0^2} & 0 \\ \frac{\sqrt{2}f^2}{s-m_0^2} & \frac{f^2}{s-m_0^2} & \frac{f^2}{s-m_0^2} & 0 \\ \frac{f^2}{s-m_0^2} & \frac{f^2}{s-m_0^2} & \frac{f^2}{s-m_0^2} & 0 \\ 0 & 0 & 0 & \frac{2f^2}{s-m_{\eta}^2} + \frac{f^2}{s-m_{\eta'}^2} + \frac{f^2}{s-m_{\eta_c}^2} \end{bmatrix}$$

with

$$P = \begin{bmatrix} (s-m_{\pi}^2) & 0 & 0 & 0 \\ 0 & (s-m_{\pi'}^2)^{-1} & 0 & 0 \\ 0 & 0 & (s-m_{\pi_c}^2)^{-1} & 0 \\ 0 & 0 & 0 & (s-m_0^2)^{-1} \end{bmatrix}$$

where the renormalized propagator is

$$\pi^{\alpha\beta} = (P^{-1} - Q)^{-1} = \sum_i \frac{v_i^{\alpha} v_i^{\beta}}{s - m_i^2} \equiv \sum_i \frac{R_{\alpha\beta}^i}{s - m_i^2}$$

$m_i = (m_{\pi}, m_{\pi'}, m_{\pi_c}, m_0)$  are solutions of  $|\pi| = 0$ , and

$$v_i = \frac{[\sqrt{2} f (m_i^2 - m_{\pi}^2)^{-1}, f (m_i^2 - m_{\pi'}^2)^{-1}, f (m_i^2 - m_{\pi_c}^2)^{-1}, 1]}{\left(1 + \frac{2f^2}{(m_i^2 - m_{\pi}^2)^2} + \frac{f^2}{(m_i^2 - m_{\pi'}^2)^2} + \frac{f^2}{(m_i^2 - m_{\pi_c}^2)^2}\right)^{\frac{1}{2}}}$$

The fourth "0" channel represents a quarkless state which mediates the OZI violation, and is here approximated by a pole. As implemented, probability leaks into this state and we have  $4 \times 4$  orthogonality and completeness. It is possible to reformulate this problem in a physically inequivalent form with a general interaction



$$0 = h(s) \begin{bmatrix} 2 & \sqrt{2} & 1 \\ \sqrt{2} & 1 & 1 \\ 1 & 1 & 1 \end{bmatrix}$$

Since this is an energy-dependent interaction, orthogonality and completeness hold at a given value of  $s$ . Thus in evaluating the residues orthogonality is lost but completeness is realized in a  $3 \times 3$  sense. The procedure is technically complicated by subsidiary conditions on  $h(s)$  which guarantee the stability of the physical masses and the  $3 \times 3$  completeness. This will be described in detail elsewhere. The main result of this calculation is that there exists an alternative to the  $4 \times 4$  system we describe whose numerical output is the  $3 \times 3$  submatrix of the  $4 \times 4$  residue matrix, renormalized so that the diagonal residues sum to unity in the  $3 \times 3$  channel space.

Continuing with the  $4 \times 4$  theory, with  $m_{\pi\pi}^2 = m_{\pi}^2$  and  $m_{\pi\eta}^2 = 2m_k^2 - m_{\pi}^2$  specified by the ideal mixing formula, and  $m_{\eta}^2$ ,  $m_{\eta' }^2$ , and  $m_{\eta_c}^2$  determined by experiment [we take  $m_{\eta_c}^2$  to be the recently discovered state at 2.80 GeV], we find the theory is completely determined, yielding

$$f_{OP}^2 = .1916$$

$$m_{\eta_c}^2 = 2.79 \text{ GeV}$$

and the residue matrices of Table I.

With reference to the alternative  $3 \times 3$  theory discussed above, the practical effect is to drop the "0" sector, leave the  $\mathcal{R}_{\eta}$  and  $\mathcal{R}_{\eta_c}$  residues essentially unchanged, and increase all  $\mathcal{R}_{\eta'}$  residues by  $\sim 70\%$ . Effects of this difference

on our results will be noted below, where MI refers to the  $4 \times 4$  model and MII to the  $3 \times 3$  model. When the differences are small the particular model will not be identified.

### 3. Hadronic Rates

We have, referring to Fig.2a,

$$\Gamma_{\psi, \psi\eta} = \frac{P_\psi^3}{3} \frac{G_{V'VP}^2}{4\pi} R_{\eta_c \bar{\eta}_c}^\eta .$$

If, guided by the experience<sup>1,6</sup> with the vector-vector-scalar vertex which indicate  $G_{V'VS} \approx G_{VVS}$ , we assume  $G_{V'VP} \approx G_{VVP}$ , and determine  $G_{VVP}$  from (i)  $\omega \rightarrow \pi^0 \gamma$  via vector dominance, (ii)  $\omega \rightarrow 3\pi$  via Gell-Mann, Sharp, Wagner<sup>9</sup> intermediate  $\rho$  pole method, (iii) the SU(6) relation  $G_{\omega\rho\pi\pi}^2 = 4G_{\rho\pi\pi}^2/m_\rho^2$ , and (iv)  $\phi \rightarrow \rho\pi$ , as in Ref.1. All methods are consistent with  $\frac{1}{2} G_{\omega\rho\pi\pi}^2/4\pi = G_{VVP}^2/4\pi \approx 9 \pm 2$ . Then

$$\Gamma_{\psi, \psi\eta} \approx (9 \pm 2) \text{ KeV} \quad (\text{experiment}^{10} \quad 9.6 \text{ KeV}).$$

A number of other predictions follow easily:

$$\frac{\Gamma_{\psi\eta\omega}}{\Gamma_{\psi\rho\pi}} = \frac{1}{3} \frac{G_{\omega\omega\eta}^2}{G_{\omega\rho\pi}^2} \left| \frac{P_\omega}{P_\rho} \right|^3 R_{\eta\eta}^\eta \approx .03$$

$$\frac{\Gamma_{\psi\eta'\phi}}{\Gamma_{\psi\eta\omega}} \approx \left| \frac{P_\phi}{P_\omega} \right|^3 \left( \frac{m_\psi^2 - m_\omega^2}{m_\psi^2 - m_\phi^2} \right)^2 \frac{R_{\eta'\eta}^{\eta'}}{R_{\eta\eta}^\eta} \approx \left\{ \begin{array}{l} .7 \text{ (MI)} \\ 1.1 \text{ (MII)} \end{array} \right\}$$

$$\frac{\Gamma_{\psi\eta'\omega}}{\Gamma_{\psi\eta\omega}} \approx \left| \frac{P_{\eta'}}{P_{\eta}} \right|^3 \frac{\mathcal{R}_{\eta'}}{\mathcal{R}_{\eta}} \approx \left\{ \begin{array}{l} .38 \text{ (MI)} \\ .59 \text{ (MII)} \end{array} \right\}$$

An interesting way of looking for  $\eta_c$  is in the decay  $\psi' \rightarrow \eta_c \omega$ . Rosen-sweig<sup>4</sup> predicts that this rate is only slightly ( $\frac{1}{3}$ ) suppressed relative to  $\psi' \rightarrow \psi\eta$ . Within our framework, however (see Fig.2b), since the  $0^+$  OZI transitions are more copious than the  $1^-$  OZI transitions (which can be handled perturbatively) we have

$$\frac{\Gamma_{\psi'\omega\eta_c}}{\Gamma_{\psi'\psi\eta}} = \left| \frac{P_{\eta_c}}{P_{\eta}} \right|^3 \frac{2f_{OV}^4}{(m_{\omega}^2 - m_o^2)^2 (m_{\omega}^2 - m_{\psi}^2)^2} \frac{1}{\mathcal{R}_{\eta_c} \bar{\eta}_c} \approx .084$$

This model makes predictions, of course, for OZI violating production processes as well. Referring to Fig.2c, we have

$$\frac{d\sigma(\pi^- p \rightarrow \eta n)}{d\sigma(\pi^- p \rightarrow \eta' n)} = \frac{\mathcal{R}_{\eta}}{\mathcal{R}_{\eta'}} \approx \left\{ \begin{array}{l} 2.05 \text{ (MI)} \\ 1.3 \text{ (MII)} \end{array} \right\}$$

where both cross sections are evaluated at the same  $s$ ,  $t$ , and  $q^2$ . Hopefully, the extrapolation in  $q^2$  from  $m_{\eta}^2$  to  $m_{\eta'}^2$  is not too serious. However, comparisons should be made at the same  $s$  and  $t$ . We expect the predicted ratio to be much more accurate at  $t=0$ , since production processes at high momentum transfer depend more strongly on the mass of the produced object. Extensive data on this reaction will be available shortly.<sup>11</sup>

It is interesting to note that in our formalism we are able to account for the masses and the OZI suppression with physical  $\eta$  and  $\eta'$  that have extremely

small admixture of charm. In particular, referring to Table I, we find .028% charm in  $\eta$  and .16% charm in  $\eta'$ . This is in sharp contrast to the Harari<sup>2</sup> treatment. The origin of this is clear: in our treatment the OZI violation contributes to both diagonal and off-diagonal terms in the mass matrix. Thus we are freed from the constraint

$$m_{\eta}^2 + m_{\eta'}^2 + m_{\eta_c}^2 = m_{\eta}^2 + m_{\eta'}^2 + m_{\eta_c}^2$$

which forces Harari's large charm admixture.

#### 4. Photonic Rates

Also in contrast to Harari, we find no serious problems with  $\gamma$ -decays in the context of the vector dominance model. The new ingredient here, apart from a different mixing, is the use of  $\psi'$  as another intermediate state in decays involving  $\psi$  as an intermediate state.<sup>6</sup> We choose a judicious relative phase. We do not believe this is artificial because there is no reason why, consistent with the assumption  $G_{V'\gamma}^2 \approx G_{VVP}^2$  we can not have  $G_{V'\gamma} \approx -G_{VVP}$ . Moreover, alternating signs considerably enhance the possibility of a convergent generalized VDM sum. This addition of radial excitations, interesting enough, does not spoil rates like  $\omega \rightarrow \pi^0 \gamma$  since the  $\rho'$  electronic width is expected to be considerably smaller than the  $\rho$  electronic width,<sup>12</sup> in contrast to the  $\psi'$  vs.  $\psi$  electronic widths. With these preliminaries, consider the rates, referring to Figs. 2d and 2e,

$$\Gamma_{\phi \rightarrow \eta \gamma} = \frac{|P_{\gamma}|^3}{3} \frac{G_{VVP}^2}{4\pi} \frac{3\Gamma_{\phi \rightarrow e^+ e^-}}{\alpha m_{\phi}} R_{\eta, \eta'}$$

yielding a partial width of  $(44.5 \pm 10) \text{ KeV}$  consistent with recent data<sup>13</sup>

indicating an experimental partial width of  $65 \pm 15$  KeV. (Our quoted error is determined by the uncertainty in  $G_{VVP}$ .)

Similarly we have

$$\Gamma_{\varphi \rightarrow \pi^0 \gamma} = \frac{|P_Y|^3}{3} \frac{2G_{VVP}^2}{4\pi} \left( \frac{3\Gamma_{\rho e^+ e^-}}{\alpha m_\rho} \right) \frac{2f_{OV}^4}{(m_\varphi^2 - m_\pi^2)^2 (m_\varphi^2 - m_\omega^2)^2}$$

yielding a partial rate of  $(10.8 \pm 3)$  KeV compared with the experimental<sup>13</sup> partial rate of  $5.9 \pm 2.1$  KeV.

Referring to Fig.2f, with  $\psi_I$  now  $\psi$  and  $\psi'$ , we have for  $\psi \rightarrow \eta \gamma$ ,

$$\begin{aligned} \Gamma_{\psi \eta \gamma} &= \frac{1}{4\pi} \frac{|P_Y|^3}{3} \left| \mathcal{R}_{\eta_c \bar{\eta}_c}^\eta \left[ \frac{eF_\psi}{m_\psi} G_{VVP} + \frac{eF_{\psi'}}{m_{\psi'}} G_{V'VP} \right] \right|^2 \\ &= \frac{|P_Y|^3}{3} \frac{G_{VVP}^2}{4\pi} \mathcal{R}_{\eta_c \bar{\eta}_c}^\eta \frac{3\Gamma_{\psi e^+ e^-}}{\alpha} \frac{1}{m_\psi} \cdot B \end{aligned}$$

where

$$B = \left( 1 + \frac{G_{VV'P}}{G_{VVP}} \sqrt{\frac{\Gamma_{\psi' e^+ e^-} m_\psi}{\Gamma_{\psi e^+ e^-} m_{\psi'}}} \right)^2$$

Using  $\Gamma_{\psi \eta \gamma} = 100 \text{ eV}^{15}$  we find that

$$\frac{G_{VV'P}}{G_{VVP}} = -1.24, -1.98$$

with the first root consistent with our earlier assumption<sup>14</sup>  $G_{VV'P}^2 \approx G_{VVP}^2$ .

Using this new determination we have

$$\Gamma_{\psi\eta_c\gamma} = \frac{|P_Y|^3}{3} \frac{G_{VVP}^2}{4\pi} \frac{\eta_c}{\eta_c \bar{\eta}_c} \frac{3\Gamma_{\psi e^+ e^-}}{\alpha} \frac{1}{m_\psi} B = 2.2 \text{ KeV}$$

which is now a prediction based on  $\Gamma_{\psi\eta\gamma}$ .

Similarly we find

$$\frac{\Gamma_{\psi\eta'\gamma}}{\Gamma_{\psi\eta\gamma}} = \begin{array}{ll} 4.6 & \text{(MI)} \\ 7.5 & \text{(MII)} \end{array} \quad (\text{data}^{13} 4 \pm 2.5)$$

Treating the  $\psi' \rightarrow \eta_c \gamma$  decay in analogy to the  $\psi \rightarrow \eta_c \gamma$  decay we find

$$\Gamma_{\psi'\eta_c\gamma} = \frac{|P_Y|^3}{3} \frac{G_{VV'P}^2}{4\pi} \frac{\eta_c}{\eta_c \bar{\eta}_c} \frac{3\Gamma_{\psi' e^+ e^-}}{\alpha} \frac{1}{m_{\psi'}} B'$$

where

$$B' = \left| 1 + \frac{G_{V'V'P}}{G_{VV'P}} \sqrt{\frac{\Gamma_{\psi' e^+ e^-} m_\psi}{\Gamma_{\psi e^+ e^-} m_{\psi'}}} \right|^2$$

If we assume  $G_{VVP} G_{V'V'P} \approx G_{VV'P}^2$

$$\Gamma_{\psi'\eta\gamma} \approx 50 \text{ KeV.}$$

Continuing in this spirit,

$$\begin{aligned} \Gamma_{\eta_c \rightarrow \gamma\gamma} &= \frac{G_{VVP}^2}{4\pi} \frac{|P_Y|^3}{2} \left( \frac{3\Gamma_{\psi e^+ e^-}}{\alpha m_\psi} \right)^2 \\ &\times \left[ 1 + \frac{\Gamma_{\psi m_\psi} G_{VV'P}^2}{\Gamma_{\psi m_\psi} G_{VVP}^2} + 2 \frac{G_{VV'P}}{G_{VVP}} \sqrt{\frac{\Gamma_{\psi' e^+ e^-} m_\psi}{\Gamma_{\psi e^+ e^-} m_{\psi'}}} \right]^2 \cong 15 \text{ eV.} \end{aligned}$$

(This width should be taken with caution since it depends on the square of the difference of two large numbers; a factor of two variation in the coupling ratio can result in a factor of 50 increase in the rate.)

Taking  $\Gamma_{\eta_c}$  full width to be 100 KeV, certainly a lower limit, we find

$$\frac{\Gamma_{\psi' \eta_c \gamma}}{\Gamma_{\psi'}} \frac{\Gamma_{\eta_c \gamma \gamma}}{\Gamma_{\eta_c}} \leq 4 \times 10^{-5}$$

which is well within the experimental<sup>15</sup> bound.

Finally, consider  $\psi' \rightarrow \rho_0 \rho_0 \gamma$ , which Harari points out may be a possible problem. We have

$$\Gamma_{\psi' \rightarrow \rho_0 \rho_0 \gamma} \leq \Gamma_{\psi' \rightarrow \gamma \eta_c} B_{\eta_c \rho_0 \rho_0} = 50 \text{ KeV} \quad B_{\eta_c \rho_0 \rho_0} \leq 7 \text{ KeV, experiment}^{16}$$

which is consistent with a plausible branching ratio  $B_{\eta_c \rho_0 \rho_0}$  for  $\eta_c \rightarrow \rho_0 \rho_0$ .

Our decay rates are summarized in Table II.

## 5. Summary and Conclusions

We find

(i) The mixing generated by O-meson or cylinder correction, controlled by the  $0^-$  masses, yields a correct rate for  $\psi' \rightarrow \psi \eta$  and results in predictions for a number of measurable hadronic rates, different from the predictions of Rosenzweig.<sup>4</sup>

(ii) The admixture of charm in  $\eta$  and  $\eta'$  is much smaller than the model of Harari indicates.

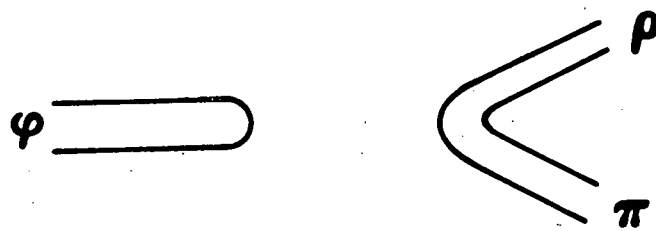
(iii) The photonic rates, calculated using this mixing and the extended VDM, yield results consistent with experiment.

## References

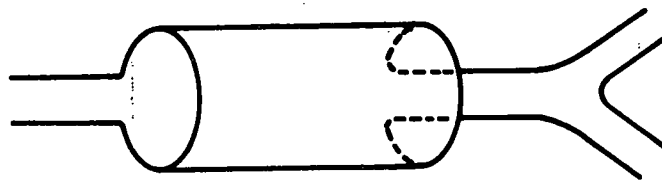
1. J. F. Bolzan, K. A. Geer, W. F. Palmer, and S. S. Pinsky, Phys. Rev. Lett. 35, 419 (1975); Phys. Lett. 59B, 351 (1975); OSU preprint C00-1545-171; S. Pinsky and D. Snider, ANL-HEP-PR-75-37, Phys. Rev. D (to be published).
2. H. Harari, WIS-75/39 Ph. (Weizmann Institute).
3. M. Machacek and Y. Tomozawa, UM HE 75-32 (revised). (Univ. of Michigan).
4. C. Rosenzweig, PITT-156.
5. Chan Hong-Mo, Ken-ichi Konishi, J. Kwiecinski, and R. G. Roberts, RL-75-192/T.148. (Rutherford Lab.).
6. L. Clavelli and S. Nussinov, T.R. 76-013. (Univ. of Maryland).
7. P. G. O. Freund and Y. Nambu, Phys. Rev. Lett. 34, 1645 (1975).
8. G. Veneziano, Phys. Lett. 52B, 220 (1974); Nucl. Phys. B74, 365 (1974).
9. M. Gell-Mann, M. D. Sharp, and W. G. Wagner, Phys. Rev. Lett. 8, 261 (1962).
10. W. Tanenbaum et al., SLAC-PUB-1696; LBL-4642.
11. Data of 6.0 and 8.4 GeV<sup>2</sup> are in the final stages of analysis, private communication, N. Stanton.
12. E. P. Tryon, Phys. Rev. Lett. 36, 458 (1975).
13. C. Bemporad, Proceeding 1975 International Symposium on Lepton and Photon Interactions at High Energies, Stanford University (1975).
14. We consider this as a determination of the relative sign of  $G_{VV',P}$  and  $G_{VVP}$  but only an approximate verification of our assumption  $G_{VV',P}/G_{VVP} = 1$ , since the expression B is extremely sensitive to the vector dominance model continuation for  $q^2 = 0$  to  $m_\psi^2$ .



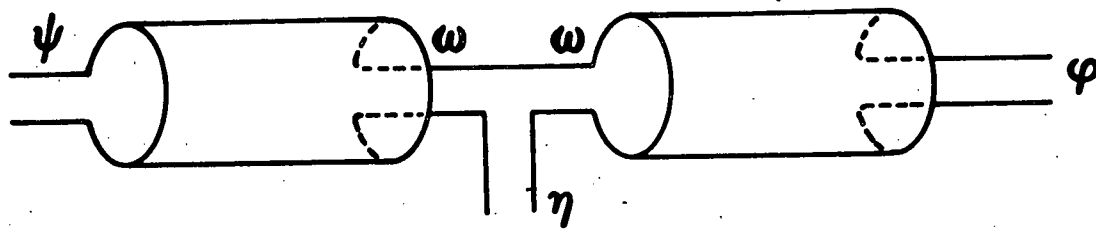
15. B. H. Wiik, Proceedings 1975 International Symposium on Lepton and Photon Interactions at High Energies, Stanford Univ. (1975).
16. J. Heintze, Proceedings 1975 International Symposium on Lepton and Photon Interactions at High Energies, Stanford Univ. (1975).



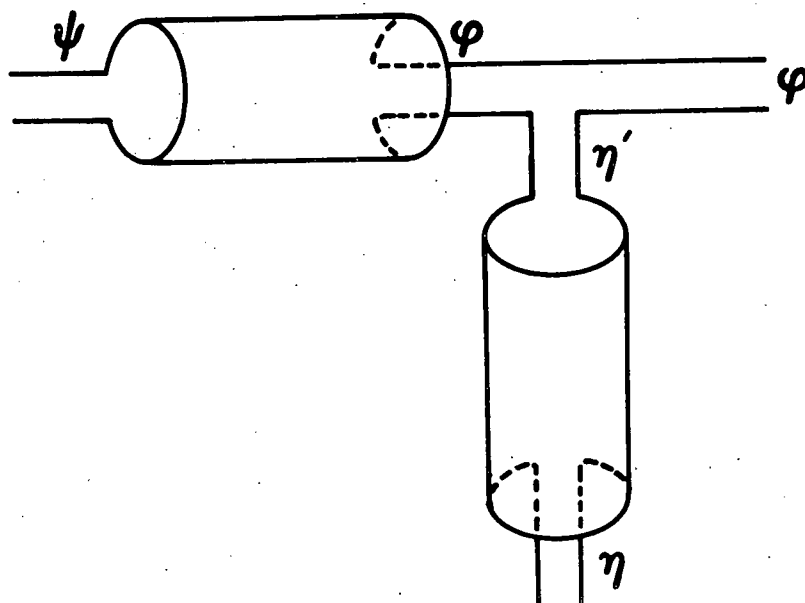
(a)



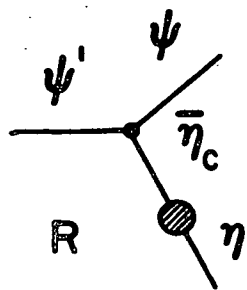
(b)



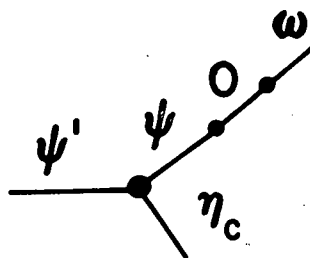
(c)



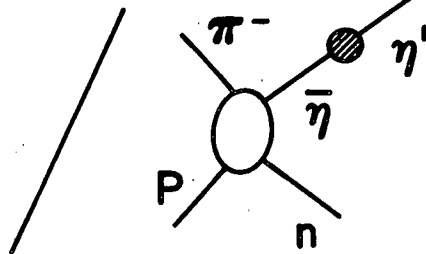
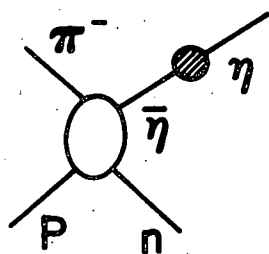
(d)



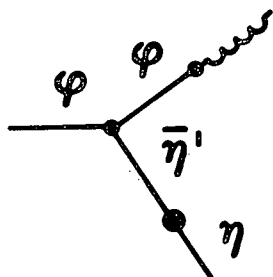
(a)



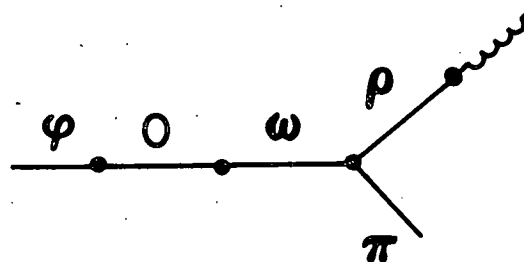
(b)



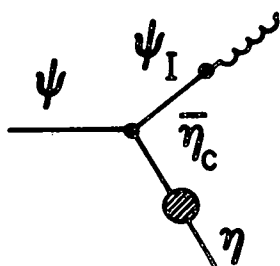
(c)



(d)



(e)



(f)

Table I

$$R^{\eta} = \begin{bmatrix} .39 & -.45 & -.010 & .18 \\ & .53 & .012 & -.21 \\ & & 2.8 \times 10^{-4} & 4.7 \times 10^{-3} \\ & & & 8.1 \times 10^{-2} \end{bmatrix}$$

$$R^{\eta'} = \begin{bmatrix} .19 & .28 & -.018 & .28 \\ & .40 & -.026 & .40 \\ & & .16 \times 10^{-2} & -.026 \\ & & & .41 \end{bmatrix}$$

$$R^{\eta_c} = \begin{bmatrix} 2.03 \times 10^{-5} & 1.5 \times 10^{-5} & 4.5 \times 10^{-3} & 2.6 \times 10^{-4} \\ & 1.1 \times 10^{-5} & 3.4 \times 10^{-3} & 1.9 \times 10^{-4} \\ & & .997 & 5.7 \times 10^{-2} \\ & & & 3.2 \times 10^{-3} \end{bmatrix}$$

Table II

Rates	Theory	Exp.
$\Gamma(\psi' \rightarrow \psi \eta)$	$9 \pm 2 \text{ KeV}$	$9.6 \pm 1.8 \text{ KeV}$
$\Gamma(\psi \rightarrow \eta \omega) / \Gamma(\psi \rightarrow \rho \pi)$	.03	
$\Gamma(\psi \rightarrow \eta' \varphi) / \Gamma(\psi \rightarrow \eta \omega)$	0.7 (MI) 1.1 (MII)	
$\Gamma(\psi' \omega \eta_c) / \Gamma(\psi' \psi \eta)$	.38 (MI) .59 (MII)	
$\Gamma(\psi' \omega \eta_c) / \Gamma(\psi' \psi \eta)$	.084	
$d\sigma(\pi^- p \rightarrow \eta n) / d\sigma(\pi^- p \rightarrow \eta' n)$	2.05 (MI) 1.3 (MII)	
$\Gamma(\varphi \rightarrow \eta \gamma)$	$44.5 \pm 10 \text{ KeV}$	$65 \pm 15 \text{ KeV}$
$\Gamma(\varphi \rightarrow \pi^0 \gamma)$	$10.8 \pm 3 \text{ KeV}$	$5.9 \pm 2.1 \text{ KeV}$
$\Gamma(\psi \eta \gamma)$	normalization	$100 \pm 25 \text{ eV}$
$\Gamma(\psi \eta_c \gamma)$	2.2 KeV	
$\Gamma(\psi \eta' \gamma) / \Gamma(\psi \rightarrow \eta \gamma)$	4.6 (MI) 7.5 (MII)	$4 \pm 2.5$
$\Gamma(\psi' \eta_c \gamma)$	50 KeV	
$\Gamma(\eta_c \rightarrow \gamma \gamma)$	15 eV	
$\Gamma(\psi' \rightarrow \rho_0 \rho_0 \gamma)$	$< 50 B(\eta_c \rightarrow \rho_0 \rho_0) \text{ KeV}$	$< 7 \text{ KeV}$

## Figure Captions

Fig.1. (a) Dual diagram for  $\varphi \rightarrow \rho\pi$ ; (b) Equivalent cylinder diagram;  
(c) and (d) Equivalent topological diagrams for  $\psi \rightarrow \varphi\eta$ .

Fig.2. Diagrams for various OZI forbidden processes.

## Table Captions

Table I. Residue matrices for  $\eta$ ,  $\eta'$ , and  $\eta_c$  poles in the  $4 \times 4$  model (MI).

Table II. Table of various rates involving OZI forbidden transitions.

MI is the  $4 \times 4$  model and MII is the  $3 \times 3$  model.